*Protein Science* (1997), 6:2548–2560. Cambridge University Press. Printed in the USA.


# Cross-strand side-chain interactions versus turn conformation in β-hairpins

EVA DE ALBA, MANUEL RICO, AND M. ANGELES JIMÉNEZ

Instituto de Estructura de la Materia, Consejo Superior de Investigaciones Científicas, Serrano 119, 28006-Madrid, Spain

(RECEIVED March 31, 1997; ACCEPTED August 8, 1997)

**Abstract**

A series of designed peptides has been analyzed by $^1$H-NMR spectroscopy in order to investigate the influence of cross-strand side-chain interactions in β-hairpin formation. The peptides differ in the N-terminal residues of a previously designed linear decapeptide that folds in aqueous solution into two interconverting β-hairpin conformations, one with a type I turn (β-hairpin 4:4) and the other with a type I + G1 β-bulge turn (β-hairpin 3:5). Analysis of the conformational behavior of the peptides studied here demonstrates three favorable and two unfavorable cross-strand side-chain interactions for β-hairpin formation. These results are in agreement with statistical data on side-chain interactions in protein β-sheets. All the peptides in this study form significant populations of the β-hairpin 3:5, but only some of them also adopt the β-hairpin 4:4. The formation of β-hairpin 4:4 requires the presence of at least two favorable cross-strand interactions, whereas β-hairpin 3:5 seems to be less susceptible to side-chain interactions. A protein database analysis of β-hairpins 3:5 and β-hairpins 4:4 indicates that the former occur more frequently than the latter. In both peptides and proteins, β-hairpins 3:5 have a larger right-handed twist than β-hairpins 4:4, so that a factor contributing to the higher stability of β-hairpin 3:5 relative to β-hairpin 4:4 is due to an appropriate backbone conformation of the type I + G1 β-bulge turn toward the right-handed twist usually observed in protein β-sheets. In contrast, as suggested previously, backbone geometry of the type I turn is not adequate for the right-handed twist. Because analysis of buried hydrophobic surface areas on protein β-hairpins reveals that β-hairpins 3:5 bury more hydrophobic surface area than β-hairpins 4:4, we suggest that the right-handed twist observed in β-hairpin 3:5 allows a better packing of side chains and that this may also contribute to its higher intrinsic stability.

**Keywords:** β-hairpin conformation; β-sheet twist; β-turn; NMR; peptide design; protein folding; side-chain interactions

The mechanism by which a polypeptide chain folds into its native three-dimensional structure is still an open question. One of the proposed mechanisms, the framework model, includes secondary structure formation in the early steps of protein folding (Kim & Baldwin, 1990; Dyson & Wright, 1991, 1993). Extensive work on the conformational properties of protein fragments and designed peptides has been performed to gain insights into the factors responsible for the formation of secondary structure. A large body of information is now available about α-helix formation and stability (Scholtz & Baldwin, 1992; Lyu et al., 1993; Zhou et al., 1993, 1994; Muñoz & Serrano, 1994a; Baldwin, 1995), and the major principles governing the process are beginning to be understood. In contrast, very little is known about the formation of β-sheets, probably due to the high tendency of the potential β-sheet-forming peptides to aggregate. The smallest structural domain having the characteristics of an antiparallel β-sheet is a β-hairpin, i.e., two β-strands connected by a loop region with a number of interstrand backbone hydrogen bonds. β-Hairpin motifs commonly found in protein structures have been classified on the basis of the conformations adopted by the loop connecting the β-strands, both in terms of the number of residues taking part in the turn, as well as the number of interstrand hydrogen bonds between the residues flanking the turn (Sibanda & Thornton, 1991). The most abundant β-hairpin structures are those having two residues in the turn, with flanking residues forming two backbone hydrogen bonds (β-hairpins 2:2); next come loops involving three residues, with only one backbone hydrogen bond between flanking residues (β-hairpins 3:5); and finally there are those having four residues in the loop, again with two backbone hydrogen bonds between distal residues (β-hairpins 4:4) (Sibanda & Thornton, 1991). β-Hairpin structures with longer loops are very scarce (Sibanda et al., 1989). Normally, β-hairpins 2:2 have type I′ β-turns, whereas the conformations of

Reprint requests to: M. Angeles Jiménez, Instituto de Estructura de la Materia, Consejo Superior de Investigaciones Científicas, Serrano 119, 28006 Madrid, Spain; e-mail: angeles@malika.iem.csic.es.

*Abbreviations:* δ, proton chemical shift; $\Delta\delta_{C\alpha H}$, CαH conformational shift; ASA, accessible surface area; $M_{av}$, averaged molecular weight; $M_{th}$, theoretical molecular weight; NOESY, NOE spectroscopy; ROESY, rotating frame NOE spectroscopy; TOCSY, total correlation spectroscopy.

β-hairpins 3:5 and 4:4 are more frequently found having a type I + G1 β-bulge turn and a regular type I turn, respectively (Sibanda & Thornton, 1991).

Some peptides containing non-natural amino acids (Haque et al., 1994, 1996) as well as nonpeptide scaffolds able to bring the two strands together (LaBrenz & Kelly, 1995; Nesloney & Kelly, 1996; Nowick et al., 1996a, 1996b) were designed with the purpose of studying β-hairpin formation. However, as far as we know, no stabilizing interstrand side-chain interactions were identified in these model systems. Recently, some protein fragments were shown to adopt β-hairpin structures in either aqueous solution (Blanco et al., 1994b) or alcohol-water mixtures (Cox et al., 1993; Blanco et al., 1994a; Searle et al., 1996) and some peptides containing only natural amino acids were designed to fold into β-hairpins in aqueous solution (Blanco et al., 1993; de Alba et al., 1995, 1996; Searle et al., 1995; Ramírez-Alvarado et al., 1996). We previously identified a pH-dependent stabilizing interaction involving the first and the third residues in the turn (de Alba et al., 1995), on the basis of changes in the sequence of a β-hairpin-forming peptide in aqueous solution (Blanco et al., 1993). More recently, the NMR investigation of a series of model decapeptides having the same strand sequence but different turn sequences allowed us to demonstrate the importance of the turn residue sequence in determining the type of β-hairpin to be formed (de Alba et al., 1997). We concluded that differences in turn propensities of residues lead to changes in β-hairpin conformation even if this causes a different β-strand residue pairing and backbone–hydrogen bond register. Substitutions of some β-strand residues by Ala in another β-hairpin-forming peptide (Ramírez-Alvarado et al., 1996) were shown to hinder the formation of the β-hairpin, but the conclusions about the influence of cross-strand side-chain interactions remained unclear, because Ala has an intrinsically low propensity to be in a β-strand.

With the aim of investigating the role of the interstrand side-chain interactions in β-hairpin formation, we analyze in this paper the conformational properties of a series of peptides (Fig. 1) derived from the model system used in our previous studies: peptide 1 in Figure 1 (de Alba et al., 1996, 1997). In the peptides studied, the residues in the β-turn and the C-terminal β-strand sequence of peptide 1 are unchanged, whereas specific residue substitutions are introduced in selected positions of the N-terminal β-strand (Fig. 1). To minimize effects due to the differences in intrinsic β-sheet propensities, all the residues involved in the substitutions have high β-sheet propensities. Analysis of the conformational properties of these peptides has allowed the detection of stabilizing cross-strand interactions as well as the determination of the relative stabilities of the two different types of β-hairpin. The results obtained agree with statistical analysis of cross-strand interactions and β-hairpin structures.

| | | β-strand residues | | | | | | | | | |
|---|---|---|---|---|---|---|---|---|---|---|---|
| | | turn residues | | | | | | | | | |
| model peptide | Peptide 1 | I1 | Y2 | S3 | N4 | S5 | D6 | G7 | T8 | W9 | T10 |
| designed peptides | Peptide 2 | S1 | Y2 | I3 | N4 | S5 | D6 | G7 | T8 | W9 | T10 |
| | Peptide 3 | Y1 | I2 | S3 | N4 | S5 | D6 | G7 | T8 | W9 | T10 |
| | Peptide 4 | S1 | Y2 | S3 | N4 | S5 | D6 | G7 | T8 | W9 | T10 |
| | Peptide 5 | Y1 | I2 | T3 | N4 | S5 | D6 | G7 | T8 | W9 | T10 |
| | Peptide 6 | Y1 | Y2 | T3 | N4 | S5 | D6 | G7 | T8 | W9 | T10 |
| | Peptide 7 | T1 | I2 | S3 | N4 | S5 | D6 | G7 | T8 | W9 | T10 |

**Fig. 1.** Peptide sequences. Turn residues in β-hairpin 4:4 are boxed. T8 belongs to the turn in β-hairpin 3:5.

## Results

### *Peptide design*

Peptide 1 (Fig. 1) folds into two almost equally populated β-hairpin conformations (de Alba et al., 1996). One is a β-hairpin 4:4 containing a type I turn (Fig. 2A) and the other is a β-hairpin 3:5 containing a type I + G1 β-bulge turn (Fig. 2B). Peptide 1 is then a good model to investigate cross-strand side-chain interactions, because a given mutation in its sequence would provide information simultaneously about two different cross-strand pairings (one in each of the two conformations) as well as on the importance of cross-strand interactions in two different types of β-hairpin.

All substitutions were on the N-terminal strand of the hairpin. Each residue substitution introduced in a β-strand modifies one cross-strand interaction and, in addition, affects the β-hairpin population as a consequence of the differences in intrinsic β-sheet propensities. Thus, to discriminate between the two effects and confirm the influence of the cross-strand pair interactions in the β-hairpin stability, two peptides (peptides 2 and 3 in Fig. 1) with the same amino acid composition as peptide 1 but different sequence order were analyzed. Peptides 2 and 3 have different cross-strand interactions, but intrinsic β-strand propensities are the same, so that changes observed in the population of the β-hairpin can be ascribed solely to cross-strand interactions. Because, in contrast to peptide 1, no population of β-hairpin 4:4 was detected for peptides 2 and 3 (Table 1), one or more individual cross-strand interactions can be stabilizing β-hairpin 4:4 in peptide 1. With the aim of investigating the existence of such putative favorable cross-strand interactions, peptides 4–7 (Fig. 1) with substitutions in residues at the N-terminal strand of peptides 1–3 were designed. Pair comparison among peptides 1–7 was helpful in identifying some β-hairpin-stabilizing cross-strand interactions.

### *Aggregation test*

1D $^1$H NMR spectra acquired at 0.1 mM peptide concentration or at 2 mM (for peptide 2) or 5 mM (peptides 3–7) are identical in

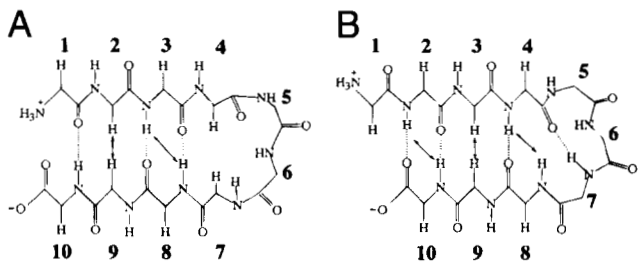


**Fig. 2.** Schematic representation of the peptide backbone conformations of a β-hairpin 4:4 with a type I β-turn (**A**) and a β-hairpin 3:5 with a type I + G1 β-bulge turn (**B**). Dotted lines indicate the β-sheet hydrogen bonds and black arrows indicate the normally observed long-range NOEs involving backbone protons. A pair of facing residues is in a hydrogen bonded site when their CO and NH are hydrogen bonded, for example, pairs 3–8 and 1–10 in the β-hairpin 4:4. When their CO and NH backbone atoms are not hydrogen bonded, the pair of residues belongs to a non-hydrogen bonded site, for example, pair 2–9 in β-hairpin 4:4.

**Table 1.** *Populations of the β-hairpin conformations formed by peptides 1–7 in $D_2O$ estimated as described in text (Searle et al., 1995; de Alba et al., 1996, 1997; Ramírez-Alvarado et al., 1996)*[a]

| | β-hairpin 4:4, type I turn | | | β-hairpin 3:5, type I + G1 β-bulge turn | | |
|---|---|---|---|---|---|---|
| Peptide | strand | turn | Estimated population | strand | turn | Estimated population |
| 1[b] | I1 Y2 S3 N4 S5<br>T10 W9 T8 G7 D6 | | 30 % | I1 Y2 S3 N4 S5<br>T10 W9 T8 G7 D6 | | 30 % |
| 2 | S1 Y2 I3 N4 S5<br>T10 W9 T8 G7 D6 | | non-detected | S1 Y2 I3 N4 S5<br>T10 W9 T8 G7 D6 | | 50 % |
| 3 | Y1 I2 S3 N4 S5<br>T10 W9 T8 G7 D6 | | non-detected | Y1 I2 S3 N4 S5<br>T10 W9 T8 G7 D6 | | 20 % |
| 4 | S1 Y2 S3 N4 S5<br>T10 W9 T8 G7 D6 | | 30 % | S1 Y2 S3 N4 S5<br>T10 W9 T8 G7 D6 | | 40 % |
| 5 | Y1 I2 T3 N4 S5<br>T10 W9 T8 G7 D6 | | non-detected | Y1 I2 T3 N4 S5<br>T10 W9 T8 G7 D6 | | 80 % |
| 6 | Y1 Y2 T3 N4 S5<br>T10 W9 T8 G7 D6 | | 10 % | Y1 Y2 T3 N4 S5<br>T10 W9 T8 G7 D6 | | 40 % |
| 7 | T1 I2 S3 N4 S5<br>T10 W9 T8 G7 D6 | | non-detected | T1 I2 S3 N4 S5<br>T10 W9 T8 G7 D6 | | 10 % |

[a]Values obtained were rounded to the closest decapercentile. Peptide sequences and residues belonging to the turn and strands of each β-hairpin type are indicated. Two dotted lines indicate residue pairs located in a hydrogen bonded site. A continuous line indicates pairs in a non-hydrogen bonded site.

[b]Data taken from de Alba et al. (1996).

line widths and chemical shifts, indicating the absence of aggregation. To further confirm the monomeric state of the peptides, sedimentation equilibrium experiments were performed with the concentrated samples for some of the peptides. The similarity between the average molecular weights obtained by this method and the molecular weights calculated on the basis of the amino acid composition indicate that the peptides are monomeric (peptide 2, $M_{th}/M_{av} = 0.97 \pm 0.09$; peptide 4, $M_{th}/M_{av} = 1 \pm 0.1$; peptide 5, $M_{th}/M_{av} = 0.94 \pm 0.09$; peptide 6, $M_{th}/M_{av} = 0.95 \pm 0.09$; peptide 7, $M_{th}/M_{av} = 0.97 \pm 0.09$). The monomeric state of peptide 1 was previously checked and reported (de Alba et al., 1996).

### *$^1H$ NMR analysis: Detection and identification of the β-hairpins 4:4 and 3:5*

$^1H$ NMR spectra of peptides 1–7 in aqueous solution at different pH values were assigned using the standard sequential assignment procedure (Wüthrich et al., 1984; Wüthrich, 1986). Proton chemical shifts of peptides 2–7 are available as supplementary material in the Electronic Appendix (Tables SM1–6).

Linear peptides in solution exist as conformational ensembles of transient interconverting structures, which are in fast exchange on the NMR time scale, due to the low energy barriers between minima in the $\phi$-$\psi$ conformational space. Thus, observed chemical shifts and coupling constants are averaged values over all existing conformations, and NOE connectivities belonging to all significantly populated conformations can be detected. The conformational analysis is usually simplified by reduction to two sets of structures, one set corresponding to the random coil state, and the other set to folded structures. In the discussion that follows, we refer to the set of folded structures collectively as "structure adopted by a peptide." In addition, two families of folded structures (two different types of hairpin structures, see below) are adopted in some of the peptides investigated here. The medium- and long-range NOE connectivities, with zero intensity in the random coil state, and the C$\alpha$H conformational shifts ($\Delta\delta_{C\alpha H} = \delta_{observed} - \delta_{random\ coil}$; Bundi & Wüthrich, 1979), expected to be zero in the random coil state of any peptide, are the most important NMR data indicative of structure formation. The NOEs, with their critical dependence on interproton distances, provide the most relevant structural information and allow us to distinguish between the formation of different types of β-hairpin conformation. Figure 2 is a schematic representation of the β-hairpin 4:4 and the β-hairpin 3:5 conformations expected for the peptides in this study. The two β-hairpins can be distinguished by their different NOE patterns. Thus, β-hairpin 4:4 would show NOE correlations between the NH protons of residues 3 and 8 and the C$\alpha$H protons of residues 2 and 9 (Fig. 2A), whereas, for β-hairpin 3:5, NH-NH NOEs connecting residues 2–10 and 4–8, and a C$\alpha$H3-C$\alpha$H9 NOE crosspeak would be observed (Fig. 2B).

Both NOESY and ROESY spectra were performed for all the peptides under almost all experimental conditions. The pattern of NOE crosspeaks found in the ROESY and NOESY spectra of a particular peptide under the same experimental conditions were practically identical. Joint analysis of NOESY and ROESY spectra allows a check on whether a particular crosspeak corresponds to a true NOE connectivity, because it permits one to discard the presence of spin diffusion in NOESY experiments and of other artefacts in ROESY spectra. Thus, cross-correlations observed in the ROESY spectra and, in most cases, also in the NOESY spectra, are referred to below. In order to identify the type of β-hairpin adopted by the peptides, both types of spectra provide the same structural information.

The C$\alpha$H conformational shifts are expected to be negative in the turn region and positive in the β-strand regions (Case et al., 1994; Wishart & Sykes, 1994), although the presence of aromatic residues can perturb this rule because of ring current effects. Nevertheless, the conformational shifts are, in general, useful parameters to support the formation of β-hairpin structures. Because the $\phi$ and $\psi$ angles of the first residue of the turn (residue N4 in these peptides) in a β-hairpin 3:5, containing a turn of type I + G1 β-bulge, are located in the $\beta$ region of the Ramachandran map (Sibanda & Thornton, 1991), the $\Delta\delta_{C\alpha H}$ expected for N4 should be positive. In contrast, when the β-hairpin 4:4 is formed, the turn is of type I and the ($\phi$,$\psi$) angles of residue N4 are in the $\alpha_R$ region of this map (Sibanda & Thornton, 1991), so that its $\Delta\delta_{C\alpha H}$ is expected to be negative. When both conformations are present, a weighted average value of the $\Delta\delta_{C\alpha H}$ of residue N4 would be observed. Residues in the β-strands should have similar $\phi$ and $\psi$ angles in both β-hairpin conformations, so that their $\Delta\delta_{C\alpha H}$ will be helpful in supporting the formation of β-hairpin structures, but not in discriminating between the two types of β-hairpins.

### *Peptides 2, 3, 5, and 7 form only one β-hairpin conformation (β-hairpin 3:5) in aqueous solution*

Peptides 2, 3, 5, and 7 present a unique CαH-CαH NOE crosspeak corresponding to the one between residues 3 and 9 (Fig. 3A) and NH-NH NOEs between residues 2 and 10 and 4 and 8 (Table 2; the NH4-NH8 NOE for peptide 3 is not observed), which indicates the formation of a single β-hairpin conformation, the β-hairpin 3:5 (Fig. 2B). In peptides 2 and 5, the observed NOE cross-peak connecting the NH proton of residue N4 with the CαH proton of residue W9 is a further indication of the formation of the β-hairpin 3:5 (see Tables SM7 and SM10). In peptides 3 and 7, this NOE was not detected, probably due to their lower β-hairpin population (Table 1). Additional NOEs connecting the side-chain protons of residues that face each other in the β-hairpin 3:5 support the formation of this structure, for example, the NOEs between the side chains of residues Y2–T10 and I3–W9 in peptide 2 (Fig. 3B; Table SM7), residues S3–W9 and Y1–W9 (residues not facing each other, but with side chains on the same side of the β-sheet) in peptide 3 (Fig. 3B; Table SM8), residues I2–T10 (Table SM10), T3–W9, and Y1–W9 in peptide 5 (Fig. 3B; Table SM10), and residues S3–W9 and T1–W9 in peptide 7 (Fig. 3B; Table SM12). In brief, peptides 2, 3, 5, and 7 in aqueous solution adopt a β-hairpin 3:5 conformation, which is interconverting in fast dynamic equilibrium with random coil conformations.

The $\Delta\delta_{C\alpha H}$ profiles of peptides 2, 3, 5, and 7 support the presence of a unique β-hairpin conformation. The negative values of the $\Delta\delta_{C\alpha H}$ of residues 5, 6, and 7 are indicative of the chain-bend region, and the positive conformational shifts of the CαH proton of residue 4 (Fig. 4) indicate the formation of the β-hairpin 3:5, as discussed above. The positive value of the $\Delta\delta_{C\alpha H}$ of residues 2, 8, and 9 (and also of residue 3 in peptide 5) supports the location of these residues in the β-strands. Despite being located in the β-strand, the CαH proton of the residue 3 in peptides 2, 3, and 7 show negative conformational shifts, as previously found in peptide 1 (de Alba et al., 1996). This is probably due to their proximity, and hence susceptibility to the ring current effects of W9. In contrast, T3 in peptide 5 has a positive conformational shift expected for a residue in a β-strand and may indicate a spatial orientation for this residue different from that in the other peptides. The $\Delta\delta_{C\alpha H}$ of the residues 1 and 10 being at the ends are not useful as structural parameters.

The populations of the β-hairpin 3:5 conformation adopted by peptides 2, 3, 5, and 7, estimated on the basis of the CαH3–CαH9 NOE intensity (Searle et al., 1995; de Alba et al., 1996; Ramírez-Alvarado et al., 1996), as described in Materials and methods, are given in Table 1.

### *Peptides 1, 4, and 6 adopt different interconverting populations of β-hairpin 3:5 and 4:4 conformations in aqueous solution*

NOE patterns for peptides 4 and 6 parallel those reported previously for peptide 1 (de Alba et al., 1996). Peptides 4 and 6 show a CαH-CαH NOE cross-peak between residues 3 and 9 (see Fig. 5A), an NH-NH NOE connecting residues 2–10, and an NH-NH NOE correlation between residues 4 and 8 (this NOE is not observed for peptide 6; see Table 2), indicating the formation of the β-hairpin 3:5. In addition, peptides 4 and 6 show a strong NOE connecting the CαH protons of residues 2 and 9 (Fig. 5A) and an NH-NH NOE connecting residues 3 and 8 (again not observed for peptide 6; see Table 2). These NOEs, not compatible with the structure of a β-hairpin 3:5, are indicative of the formation of a β-hairpin 4:4 (Fig. 2A). Like peptide 1 (de Alba et al., 1996), peptides 4 and 6 also show some NOEs connecting the side chains of residues 2–9 (Fig. 5B), again indicating the formation of β-hairpin 4:4, and also NOEs indicative of the formation of the β-hairpin 3:5 conformation [see Fig. 5B and Tables SM9 and SM11 for peptides 4 and 6, respectively, and de Alba et al. (1996) for peptide 1]. In summary, peptides 1, 4, and 6 in aqueous solution adopt a mixture of two different β-hairpin conformations that are in fast dynamic equilibrium with random coil conformations.

The $\Delta\delta_{C\alpha H}$ of almost all residues of peptides 1, 4, and 6 are very similar to those obtained for peptides 2, 3, 5, and 7 with the exception of residue N4, whose conformational shift is small but negative (Fig. 4). This is probably due to the simultaneous presence of β-hairpin 4:4 and β-hairpin 3:5 conformations. As previously mentioned, positive and negative values of $\Delta\delta_{C\alpha H}$ for residue N4 are expected for β-hairpins 3:5 and 4:4, respectively. Therefore, because these peptides are able to adopt significant populations of both β-hairpin structures, the conformational shift of N4 is averaged out. As noted earlier, peptides 2, 3, 5, and 7, in contrast to peptides 1, 4, and 6, form only the β-hairpin 3:5 conformation, and so the value of $\Delta\delta_{C\alpha H}$ for N4 is, as expected, positive.

Populations of each β-hairpin conformation estimated from the corresponding $C\alpha H_i$-$C\alpha H_j$ NOE intensity (see Materials and methods) are given in Table 1.

### *Calculation of the adopted β-hairpin structures*

Because of the conformational averaging present in peptides (see above), NOE data cannot be interpreted in terms of a unique structure. Nevertheless, the calculation of a limited number of structures compatible with NOE constraints is useful as a way to visualize the conformational properties of the favored family of structures within the conformational ensemble of a peptide. With this aim, we have performed structure calculations using the distance restrictions provided by the observed nonsequential NOEs for peptides 1–7. Intraresidue and sequential NOEs were excluded given that their intensities are the most affected by the conformational averaging, because random coil conformations contribute to their intensities. Because peptides 1, 4, and 6 populate two different β-hairpin conformations, a division of the observed nonsequential NOEs into two sets, one for each type of β-hairpin, was required prior to structure calculation. NOEs connecting backbone protons were easily classified as belonging to a particular type of β-hairpin (see above). NOEs connecting the side chains of cross-strand residues were ascribed to the β-hairpin conformation in which the residues involved in the NOE belong to the same face of the β-sheet and NOE crosspeaks between the side-chain protons of residues located in the same β-strand were included in both sets. All calculations provided a group of structures compatible with all NOE constraints. A listing of the nonsequential NOEs observed for all the peptides is given as supplementary material (Tables SM7–12). Superpositions of the 10 best calculated structures for the β-hairpin 3:5 and 4:4 adopted by peptide 2 and 4, respectively, are given in Figure 6.

## Discussion

### *β-Hairpin 4:4 and β-hairpin 3:5 formation is not interdependent*

The first thing to note when analyzing the conformational behavior of peptides 1–7 (Table 1) is that all of them form significant

populations of the β-hairpin 3:5. However, three of them (peptides 1, 4, and 6) also show the simultaneous presence of the β-hairpin 4:4 conformation. This indicates that the strand sequence has a larger effect on the formation of the β-hairpin 4:4 than of the β-hairpin 3:5 because all the differences among the peptides reside only in the N-terminal strand region. It is also noteworthy that there is no correlation between an increase in the population of β-hairpin 4:4 and a decrease in the population of β-hairpin 3:5, suggesting that the two populations are not interdependent. Thus, the population of β-hairpin 3:5 is larger in peptide 4 than in peptide 1, yet both peptides have nearly the same populations of β-hairpin 4:4 (Table 1). Neither peptide 5 nor peptide 7, with the

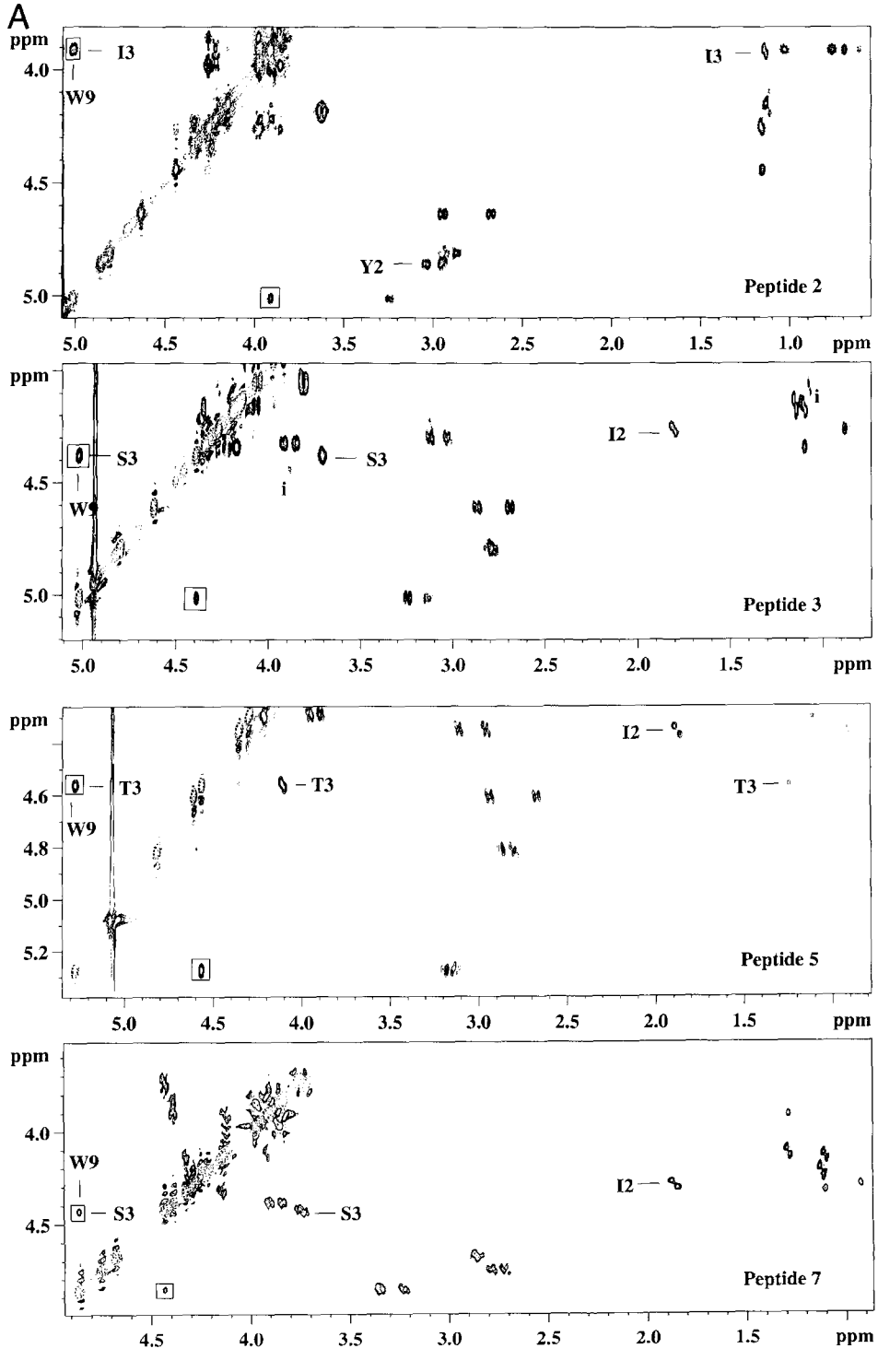

highest and the lowest populations of β-hairpin 3:5, respectively, forms a detectable population of β-hairpin 4:4 (Table 1). The simplest assumption is, therefore, that the formation of β-hairpin 4:4 and β-hairpin 3:5 are not dependent on each other, so that we can analyze the factors affecting the formation of each β-hairpin independently.

### *β-Hairpin 4:4 formation*

Because drawing conclusions from comparison of peptides differing in more than one residue is not straightforward, the best way to identify whether a particular amino acid substitution favors or hinders the formation of a β-hairpin is to compare pairs of peptides whose sequences differ in a single residue. Table 1 facilitates understanding the following discussion.

We begin comparing peptides 2 and 4, which differ only in residue 3. Although peptide 4 (with Ser 3) is able to fold into β-hairpin 4:4, peptide 2 (with Ile 3) is not (Table 1). Thus, Ser at position 3 but not Ile favors the formation of β-hairpin 4:4. This result cannot be explained in terms of differences in β-sheet propensities, because the intrinsic β-sheet propensity of Ser is lower than that of Ile (Chou & Fasman, 1974; Muñoz & Serrano, 1994b; Swindells et al., 1995). We use the statistical β-sheet propensities, because experimental β-sheet propensities obtained in host-guest studies in model proteins (Kim & Berg, 1993; Minor & Kim, 1994a; Smith et al., 1994) were shown to be context-dependent (Minor & Kim, 1994b). Consequently, the difference between peptides 2 and 4 implies that cross-strand side-chain interactions play a role in the stability of the β-hairpin 4:4 conformation of these peptides, and that the Ser 3–Thr 8 interaction (peptide 4) is favorable for its formation, whereas the Ile 3–Thr 8 (peptide 2) is unfavorable. The Ser-Thr interaction must be, then, rather effective in stabilizing the β-hairpin, because it is able to overcome the lower intrinsic β-sheet propensity of Ser with respect to Ile. Wouters and Curmi (1995) analyzed statistically side-chain interactions and pair correlations within antiparallel β-sheets, and distinguished between pairs whose backbone groups -NH and -CO are hydrogen bonded (H-bonded site), like the 3–8 pair in Figure 2A, and those whose are not. They found that the pair Ser-Thr presents a correlation larger than 1 when located in a H-bonded site, meaning that the pair occurs more frequently than expected, whereas, for the pair Ile-Thr, the correlation is smaller than 1.

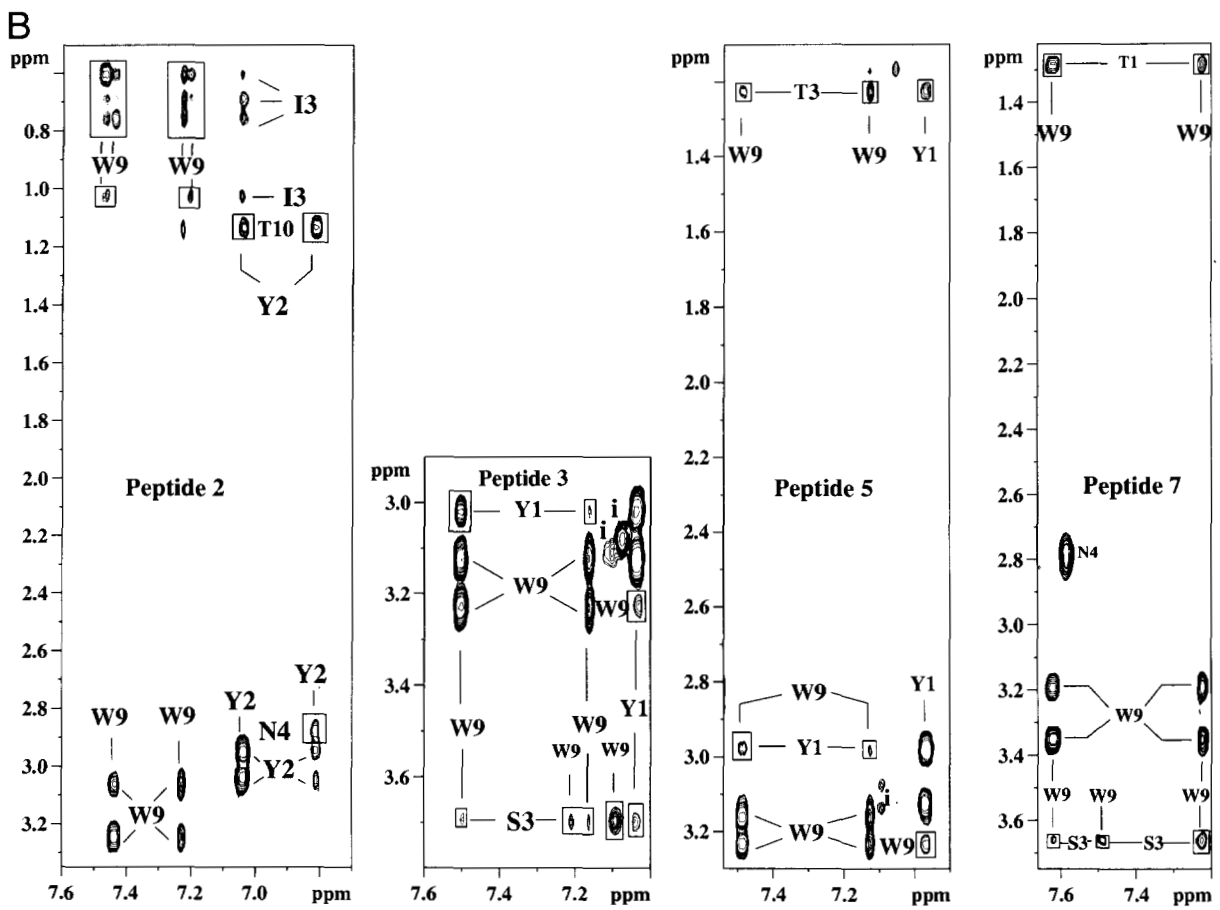


**Fig. 3.** ROESY spectra of peptides 2, 3, 4, and 5. **A:** Spectral regions showing the CαH-CαH NOEs observed for peptide 2, pH 6.3, 1 °C, 100-ms mixing time; peptide 3, pH 5.1, 12 °C, 200-ms mixing time; peptide 5, pH 6.3, 2 °C, 100-ms mixing time; and peptide 7, pH 3.7, 2 °C, 100-ms mixing time. **B:** Spectral regions showing long-range NOEs involving side-chain protons of Tyr and Trp residues found for peptide 2, pH 6.3, 1 °C, 100-ms mixing time; peptide 3, pH 5.3, 5 °C, 200-ms mixing time; peptide 5, pH 5.3, 5 °C, 200-ms mixing time; and peptide 7, pH 5.3, 2 °C, 200-ms mixing time. An impurity is denoted "I."

**Table 2.** *Intensities observed for the backbone NOEs characteristic of β-hairpin 4:4 and β-hairpin 3:5*[a]

| | β-Hairpin 4:4 | | β-Hairpin 3:5 | | |
|---|---|---|---|---|---|
| Peptide | CαH-CαH9 | NH3-NH8 | CαH3-CαH9 | NH4-NH8 | NH2-NH10 |
| 1[b] | m | w | m | m | m |
| 2 | — | — | s | w-m | m |
| 3 | — | — | m | — | w-m |
| 4 | m | vw | s | w-m | m |
| 5 | — | — | s | m | m |
| 6 | w | — | s | — | m |
| 7 | — | — | w | w | w-m |

[a]NOE intensities are classified as strong, s; medium, m; intermediate between weak and medium, w-m; weak, w; and very weak, vw; — indicates an unobserved NOE.

[b]Data taken from de Alba et al. (1996).

In contrast, for the same Ser-Ile substitution but at a different location in the sequence, in peptides 1 and 4 the β-hairpin 4:4 populations are nearly equal (Table 1). Like position 3, position 1 corresponds to an H-bonded site in the β-hairpin 4:4 (Fig. 2). Thus, the fact that the cross-strand Ser 1–Thr 10 interaction has no effect could be a consequence of being at the terminal position where end-fraying and consequently higher flexibility would be expected (de Alba et al., 1997).

If, as shown above, the substitution at position 1 does not affect the formation of β-hairpin 4:4, the differences between peptides 1 and 2 (Table 1) can be attributed solely to the β-hairpin 4:4-stabilizing cross-strand side-chain Ser 3–Thr 8 interaction in peptide 1 versus the β-hairpin-destabilizing Ile 3–Thr 8 interaction in peptide 2, as was deduced earlier between peptides 2 and 4.

Peptide 6 differs from peptide 5 only in the residue at position 2. However, peptide 6 forms β-hairpin 4:4, but peptide 5 does not do so to detectable levels (Table 1). This different conformational behavior can be attributed to the Tyr 2–Trp 9 interaction present in peptide 6 being favorable and the Ile 2–Trp 9 interaction in peptide 5 being unfavorable. Again, the Tyr-Trp interaction favors the formation of the β-hairpin 4:4, even though the intrinsic β-sheet propensity of Tyr is lower relative to Ile (Chou & Fasman, 1974; Muñoz & Serrano, 1994b; Swindells et al., 1995). This result also agrees with statistical data of cross-strand pair correlations (Wouters & Curmi, 1995), where the Tyr-Trp interaction is favorable in a non-hydrogen bonded site (Fig. 2), whereas the Ile-Trp interaction is not. Furthermore, because substitutions at position 1 do not affect β-hairpin formation (see above), comparison of peptide 3 with peptides 1 and 4, and peptide 7 with peptides 1 and 4 confirms that the Tyr 2–Trp 9 and Ile 2–Trp 9 interactions favor and disfavor, respectively, the formation of the β-hairpin 4:4, because peptides 1 and 4, where the Tyr 2–Trp 9 interaction is present, adopt the β-hairpin 4:4, whereas peptides 3 and 7, with the Ile 2–Trp 9 interaction, do not form it to a detectable population (Table 1).

The only difference between peptides 3 and 5 is the residue at position 3, but neither peptide shows any detectable population of the β-hairpin 4:4 (Table 1). Thus, the only way to determine if the Thr 3–Thr 8 interaction (present in peptides 5 and 6) is more or less favorable than the Ser 3–Thr 8 interaction for the β-hairpin 4:4 formation is by comparing peptide 6 with 1 and 4, neglecting the effect of substitution at position 1. All three peptides are able to form the β-hairpin 4:4, but the population is greater for peptides 1 and 4 (Ser 3) than for peptide 6 (Thr 3) (Table 1). Because the intrinsic β-sheet propensity of Thr is larger than for Ser (Chou & Fasman, 1974; Muñoz & Serrano, 1994b; Swindells et al., 1995), this indicates that the Thr-Thr interaction in a hydrogen bonded

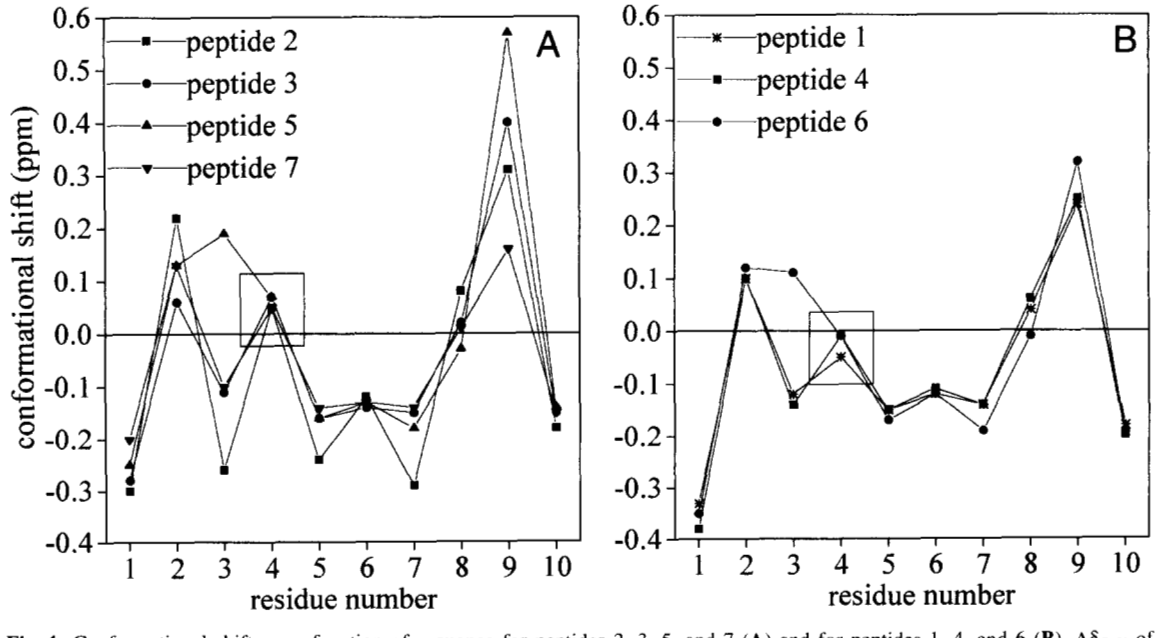


**Fig. 4.** Conformational shifts as a function of sequence for peptides 2, 3, 5, and 7 (**A**) and for peptides 1, 4, and 6 (**B**). $\Delta\delta_{C\alpha H}$ of residue 4 are boxed. For Gly, the $\Delta\delta_{C\alpha H}$ shown is with respect to the upfield-shifted CαH proton. Conformational shifts were obtained using the $\delta_{C\alpha H}$ at pH 5.3 and 5 °C, except for residue Trp 9, whose $\delta_{C\alpha H}$ was obtained under the conditions mentioned in Figures 3A and 5A for each peptide, apart from peptide 3, whose $\delta_{C\alpha H}$ (Trp 9) was taken at pH 6.3, 2 °C.

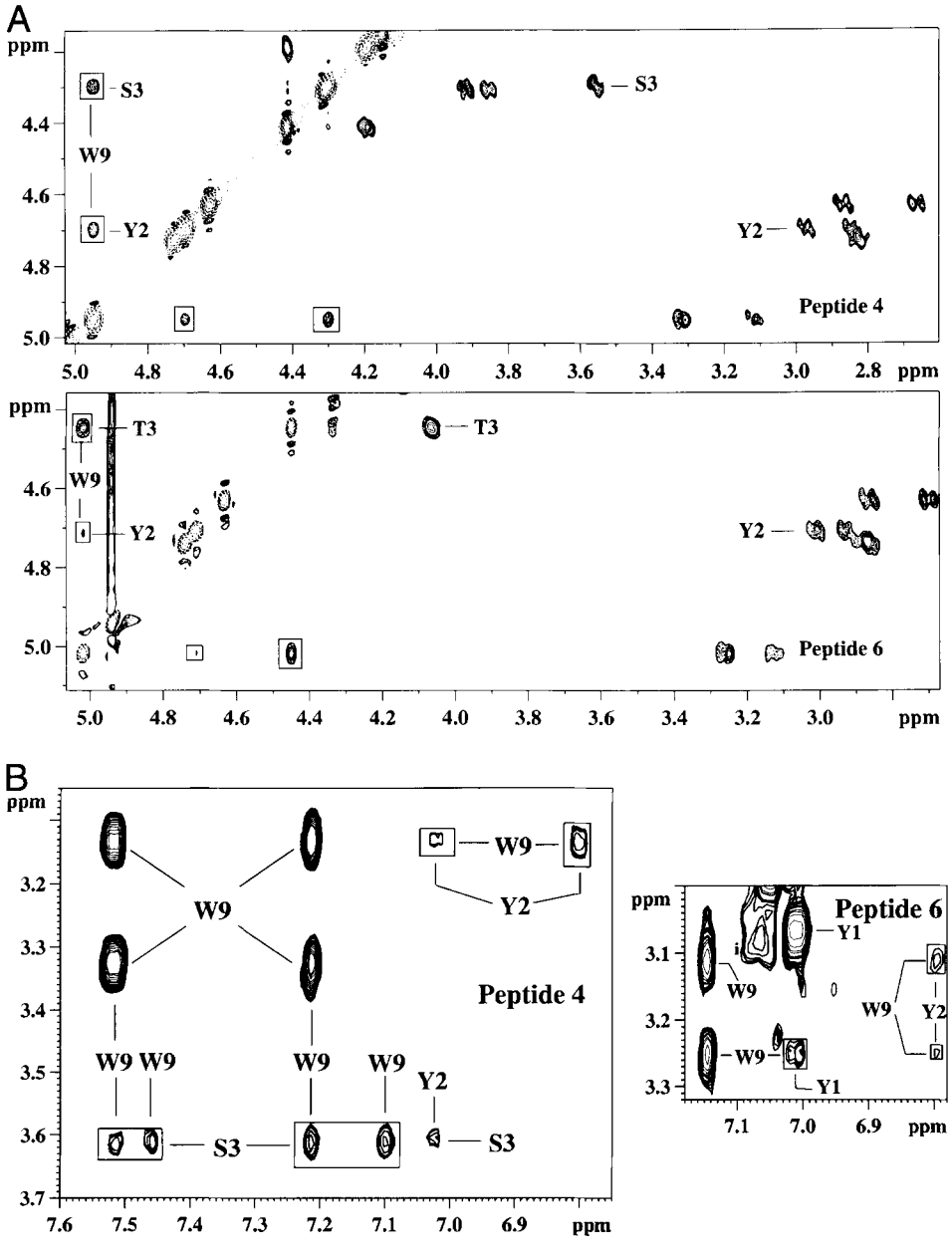


**Fig. 5.** ROESY spectra of peptides 4 and 6. **A:** Spectral region showing the CαH-CαH NOEs observed for peptide 4, pH 6.3, 2 °C, 100-ms mixing time and peptide 6, pH 6.3, 13 °C, 200-ms mixing time. **B:** Spectral regions showing long-range NOEs involving side-chain protons of Tyr and Trp residues found for peptide 4, pH 5.3, 5 °C, 200-ms mixing time and peptide 6, pH 4.3, 5 °C, 200-ms mixing time. An impurity is denoted "i."

site (Fig. 2) is less stabilizing than the Ser-Thr interaction. Because there is no effect of the substitution at position 1, the comparison of peptides 2 (Ile 3) (unable to form the β-hairpin 4:4) and 6 (Thr 3) indicates that the Thr 3–Thr 8 interaction in a hydrogen bonded site favors the formation of the β-hairpin 4:4, whereas the interaction I3–T8 destabilizes it, because Ile has a higher intrinsic β-sheet propensity than Thr (Chou & Fasman, 1974; Muñoz & Serrano, 1994b; Swindells et al., 1995). The fact that the Thr 3–Thr 8 interaction in a hydrogen bonded site is less stabilizing than the Ser-Thr is not in agreement with statistical interstrand pair correlations that consider the Thr-Thr interaction more favorable than the Ser-Thr (Wouters & Curmi, 1995). On the other hand, experimental data of interstrand side-chain interactions obtained from the comparison of the stability of protein mutants indicate that the Thr-Thr interaction is destabilizing (Smith & Regan, 1995). In our peptide system, this interaction is stabilizing, although not to the extent expected from statistical analysis (Wouters & Curmi, 1995). The discrepancies of our experimental result on the stabilizing ability of the Thr-Thr interaction with respect to both the statistical study and the experimental work by Smith and Regan (1995) may reside in the absence in our peptide model system of tertiary contacts present in a complete protein. Although Smith and Regan (1995) minimized

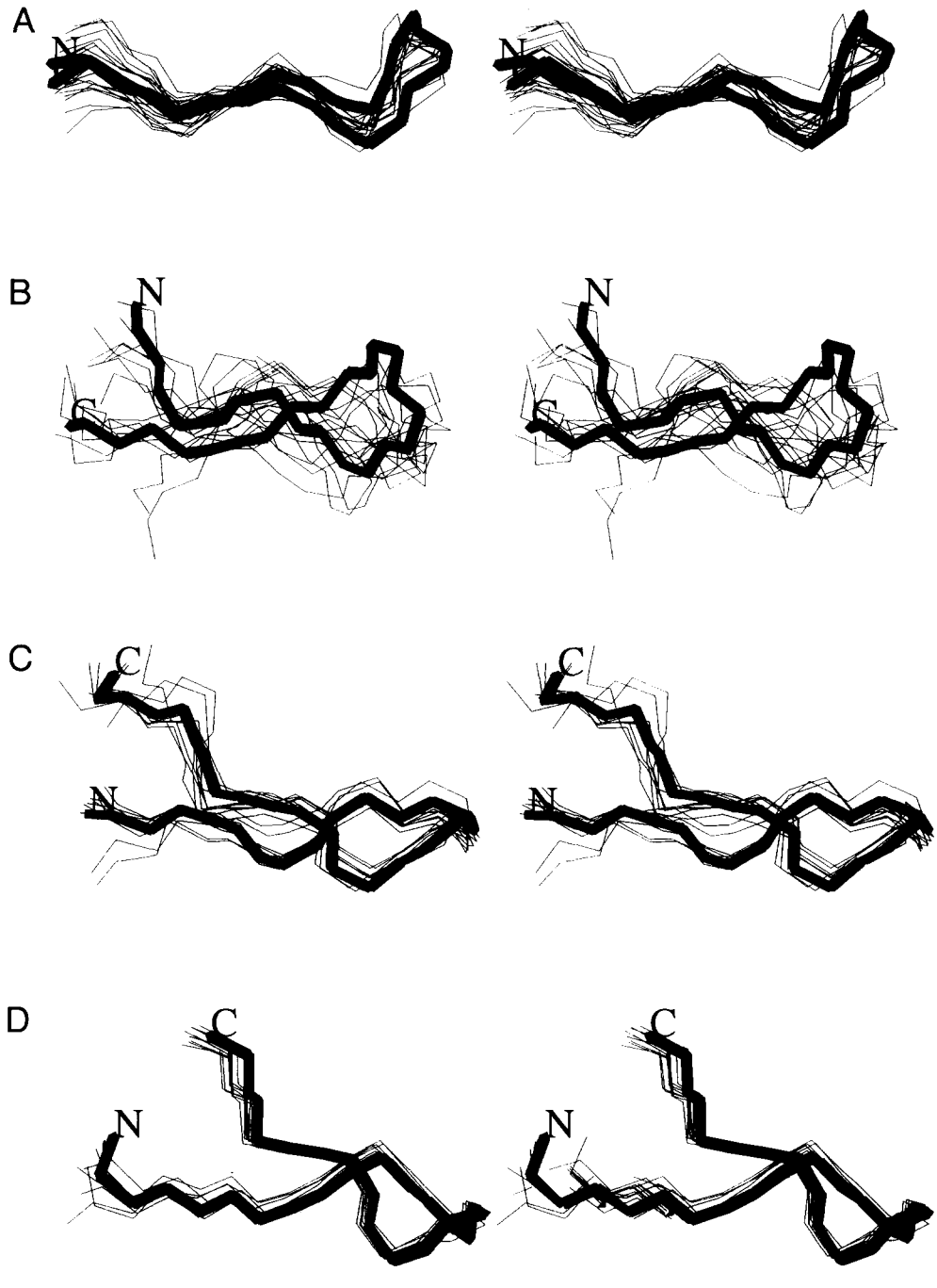


**Fig. 6.** Stereoscopic view of the superposition of the backbone atoms of (**A**) 10 segments adopting $\beta$-hairpin 4:4 conformation taken from 10 nonhomologous proteins; (**B**) the best 10 calculated structures for the $\beta$-hairpin 4:4 formed by peptide 4; (**C**) 10 segments adopting $\beta$-hairpin 3:5 conformation taken from 10 nonhomologous proteins; (**D**) the best 10 calculated structures for the $\beta$-hairpin 3:5 adopted by peptide 2.

the tertiary effects, their presence cannot be discarded completely in a protein. Our result would be, in this sense, less context-dependent. At any rate, this is the only cross-strand side-chain interaction studied on the basis of our peptide systems that deviates experimentally from what is expected from statistical data.

In short, we have identified three favorable (Ser-Thr, Tyr-Trp, Thr-Thr) and two nonfavorable (Ile-Thr, Ile-Trp) cross-strand side-chain interactions for $\beta$-hairpin formation. From the analysis of the conformational behavior of peptides 1–7 (Table 1), it is noteworthy that only those peptides with two favorable interstrand side-chain interactions (peptides 1 and 4 with the Ser-Thr, Tyr-Trp pairs and peptide 6 with the Thr-Thr, Tyr-Trp pairs; Table 1) are able to fold into a $\beta$-hairpin 4:4 conformation, whereas those lacking any of them (peptide 2 with the destabilizing Ile-Thr interaction and peptides 3, 5, 7 with the unfavorable Ile-Trp interaction) do not form significant populations of that conformation.

### *β-Hairpin 3:5 formation*

All the peptides are able to adopt the β-hairpin 3:5 conformation, but their populations are affected by the changes in the β-strand residues. In pairs of peptides differing in just a single β-strand residue (peptide 2 versus 4, 3 versus 5, and 5 versus 6), the increase in structure population correlates with a higher intrinsic β-sheet propensity of a particular residue (Chou & Fasman, 1974; Muñoz & Serrano, 1994b; Swindells et al., 1995). Thus, the population of β-hairpin 3:5 formed is significantly lower for peptide 3 (with Ser 3) than for peptide 5 (with Thr 3), in agreement with the lower intrinsic β-sheet propensity of Ser with respect to Thr. Similarly, the higher population of the β-hairpin 3:5 formed by peptide 5 (Ile 2) relative to peptide 6 (Tyr 2) agrees with the larger β-sheet intrinsic propensity of Ile with respect to Tyr. The populations of the β-hairpin 3:5 conformation adopted by peptides 2 (Ile 3) and 4 (Ser 3) are both relatively high (Table 1), but that of peptide 2 (Ile 3) is greater, in agreement with the higher intrinsic β-sheet propensity of Ile over Ser. Because the differences in the intrinsic β-sheet propensities correlate directly with the observed variation of β-hairpin 3:5 population, it is difficult, if not impossible, to evaluate separately the cross-strand side-chain interactions that modulate the β-hairpin 3:5 stability, although these cannot be neglected.

It is also worth noting the differences in the population of the β-hairpin 3:5 conformation adopted by peptides 1 and 4 (Table 1). These peptides differ only in residue 1, which lacks a cross-strand partner in the C-terminal strand. Because residue 1 is outside the β-hairpin 3:5, its backbone torsional angles will not be restricted to the β-region of the Ramachandran map. However, the population of the β-hairpin 3:5 conformation formed by peptide 4 is larger than that of peptide 1 (Table 1). The intrinsic β-sheet propensities cannot account for this result, because that of Ile (peptide 1) is higher than that of Ser (peptide 4) (Chou & Fasman, 1974; Muñoz & Serrano, 1994b; Swindells et al., 1995). A possible explanation may be that the first residue that lacks a cross-strand partner is exposed to solvent (water), interaction with which would be more favorable for a hydrophilic residue, such as Ser, than for the more hydrophobic Ile. Another explanation is the possibility of interaction of the side chain of residue 1 with that of other residues not directly facing it, although spatially proximate.

In the same way, peptides 3 and 7 differ only in the residue at position 1 and have slightly different populations of β-hairpin 3:5 (Table 1), which are not accounted for by the differences in β-sheet propensities between Tyr and Thr. The β-sheet propensity of Thr is higher than that of Tyr (Chou & Fasman, 1974; Muñoz & Serrano, 1994b; Swindells et al., 1995), but the population of β-hairpin 3:5 formed by peptide 3 (Tyr 1) is larger than that of peptide 7 (Thr 1). In this case, an explanation based on the greater hydrophobicity of Tyr over Thr is not possible, and the differences are probably the consequence of different interactions of residue 1 with nonfacing residues on the same face of the β-hairpin in the two peptides.

### *Comparison of β-hairpin 4:4 and β-hairpin 3:5 formation*

The fact that all the peptides analyzed here fold into the β-hairpin 3:5 conformation, whereas only some of them are able to adopt β-hairpin 4:4 (Table 1), suggests that type I + G1 β-bulge turns (involved in β-hairpins 3:5) are more favorable for β-hairpin formation than type I turns (β-hairpins 4:4). In a statistical study of protein structures, it was found that the great majority of β-hairpins 2:2 involve turns of type I′, with very few having type I turns, leading to the proposal that the former are more favorable for β-hairpin 2:2 formation (Sibanda & Thornton, 1985). The same rationalization may hold for type I + G1 β-bulge turns versus regular type I turns in the formation of β-hairpins 3:5 and 4:4, respectively. We therefore examined β-hairpins 3:5 and 4:4 in a protein structure database of 285 proteins using the program WHATIF (Vriend, 1990). From a total of 108 analyzed hairpins, 62% were β-hairpins 3:5 with type I + G1 β-bulge turn and 38% were β-hairpins 4:4 with a type I turn. Thus, the type I + G1 β-bulge turns are more prevalent than the type I in β-hairpins, suggesting that the former is more favorable for β-hairpin formation, as we observe in our designed peptide models. Previous studies indicated that type I turns do not have the proper geometry toward the right-handed twist commonly observed in protein β-sheets (Sibanda & Thornton, 1985; Haque et al., 1994, 1996; Haque & Gellman, 1997) and suggest why this type of turn may not be favorable for β-hairpin formation. The results obtained with our peptide systems are consistent with this suggestion. All β-hairpin 4:4 conformations adopted by our peptide models lack the right-handed twist characteristic of protein β-sheets and the protein structures show only a small or no right-handed twist (Fig. 6). In contrast, β-hairpin 3:5 conformation shows a very pronounced right-handed twist in both proteins and peptides (Fig. 6), which agrees with the statistical observation in proteins that β-bulges, in general, are usually associated with higher β-sheet twists (Chan et al., 1993). The conformational properties of the peptides studied here suggest that the different twists observed in β-hairpins 3:5 and 4:4 are a consequence of the different turn conformations present in each type of β-hairpin, the type I + G1 β-bulge turn having an appropriate geometry for the right-handed twist. This agrees with previous results indicating that the geometry of type I turns is not adequate for β-hairpin conformation.

Because the burial of hydrophobic surface was proposed as a stabilizing factor in the case of a model-designed β-hairpin 2:2-forming peptide (Ramírez-Alvarado et al., 1996), we calculated the hydrophobic surfaces buried upon formation of protein β-hairpins 3:5 and 4:4, using 10 of each type randomly selected from a protein structure database. An average of 338 $Å^2$ and 266 $Å^2$ hydrophobic surface area is buried upon the formation of β-hairpin 3:5 and β-hairpin 4:4, respectively. This result is in agreement with β-hairpins 3:5 being more stable than β-hairpins 4:4. Several theoretical studies indicate that the right-handed twist observed in protein β-sheets is mainly caused by interchain interactions within the β-sheet (Chou et al., 1985; Lasters et al., 1988; Wang et al., 1996). The relationship between the right-handed twist of β-hairpin 3:5 with a greater buried hydrophobic surface area may suggest that the right-handed twist allows a better packing of side chains and therefore makes this structure intrinsically more stable.

The formation of β-hairpin 4:4 in our peptide system needs at least two interactions between turn-flanking residues. We cannot generalize this conformational behavior to all β-hairpin 4:4-forming peptides because our peptides have only three cross-strand side-chain interactions, and that farthest from the turn is affected by fraying effects. Work with longer peptides is needed to test whether the stabilizing cross-strand side-chain interactions should necessarily involve the turn-flanking residues in a concerted action or the presence of these favorable interactions in positions farther from the turn is just enough to stabilize the β-hairpin 4:4 structure.

## Conclusion

A careful analysis of the conformational behavior of a series of β-hairpin-forming peptides having residue substitutions or a pair permutation in the sequence of β-strands has allowed us to identify some favorable cross-strand side-chain interactions (Ser-Thr and Thr-Thr in hydrogen bonded sites and Tyr-Trp in a non-hydrogen bonded site) for β-hairpin formation and some others unfavorable (Ile-Thr in a hydrogen bonded site and Ile-Trp in a non-hydrogen bonded site). These results agree with statistical data of cross-strand side-chain interactions (Wouters & Curmi, 1995). We have also demonstrated that the presence of two favorable cross-strand side-chain interactions is essential for the formation of significant populations of the β-hairpin 4:4 in the peptides reported here. The third cross-strand interaction from the turn, involving the N- and C-end residues, hardly affects the β-hairpin 4:4 stability. In contrast, the formation of β-hairpin 3:5 with a type I + G1 β-bulge turn is less susceptible to changes in the β-strand residues. These changes modify the stability of the β-hairpin 3:5, but its formation is not hindered in any of the peptides analyzed here. This suggests that the strong dependence of cross-strand side-chain interactions on β-hairpin 4:4 formation is related to an intrinsically lower stability of this structure, which in turn may be due to the presence of the type I turn. This turn, lacking the correct geometry for the right-handed twist, does not allow an optimal packing of side chains. Thus, intrinsic conformational properties of the turn backbone seem to be more important in β-hairpin conformation and stability than particular patterns of cross-strand side-chain interactions, in agreement with our previous results (de Alba et al., 1996, 1997) and those of Haque and Gellman (1997) using a different peptide system. On the basis of the structures of our peptides and those of protein β-hairpins 3:5 and 4:4, a clear relationship appears to exist between the conformation of the turn and the β-hairpin twist, in the sense that the type I + G1 β-bulge turn favors the right-handed twist, whereas the regular type I turn does not. The higher stability of β-hairpins 3:5 can be related to a better side-chain packing caused by the right-handed twist based on the greater hydrophobic surface area buried upon formation of β-hairpin 3:5.

## Materials and methods

### *Peptide synthesis and purification*

Peptides were synthesized chemically by stepwise solid-phase procedures using fluorenylmethoxycarbonyl amino acids (Coste et al., 1990), which were activated in situ using 1H-benzotriazole-1-yl-oxy-tris-pyrrolidine-phosphonium hexafluorophosphate and N-methylmorpholine as catalyst. Coupling reactions were catalyzed by 1-hydroxybenzotriazole (Atherton & Sheppard, 1989). Peptides were purified by HPLC with gradients of water (0.09% trifluoroacetic acid):acetonitrile (1% trifluoroacetic acid). Peptide purities and identities were checked by HPLC and by the complete assignment of the $^1$H-NMR spectra, respectively.

### *Sedimentation equilibrium*

Sedimentation equilibrium experiments were performed to obtain the average molecular weight of peptide samples at the concentrations used in the NMR experiments and 150 mM NaCl to screen nonideal effects involving charged residues at high peptide concentrations. Peptide samples (70 μL) were centrifuged at 40,000 rpm at 278 K in 12-mm triple-sector Epon charcoal centerpieces, using a Beckman Optima XL-A ultracentrifuge with a Ti60 rotor. Radial scans were taken at different wavelengths every 2 h until equilibrium conditions were reached. Data were analyzed using the program XLAEQ from Beckman. The partial specific volumes of the peptides at 5 °C were calculated on the basis of their amino acid composition and corrected for temperature (Laue et al., 1992). They were: 0.6964 mL/g for peptide 2; 0.6704 mL/g for peptide 4; 0.7024 mL/g for peptide 5; 0.6844 mL/g for peptide 6; and 0.6954 mL/g for peptide 7.

### *$^1$H-NMR spectra*

Peptide concentrations for NMR experiments were 2 mM for peptide 2 and 5 mM for peptides 3–7 in 0.5 mL of $H_2O/D_2O$ (9:1 ratio by volume). pH was measured with a glass micro electrode and was not corrected for isotope effects. The temperature of the NMR probe was calibrated using a methanol sample. Sodium [3-trimethylsilyl 2,2,3,3-$^2$H] propionate was used as an internal reference. The $^1$H-NMR spectra were acquired on a Bruker AMX-600 pulse spectrometer operating at a proton frequency of 600.13 MHz. One-dimensional spectra were acquired using 32K data points, which were zero-filled to 64K data points before performing the Fourier transformation. Phase-sensitive two-dimensional TOCSY (Rance, 1987), NOESY (Jeener et al., 1979; Kumar et al., 1980), and ROESY (Braunschweiler & Ernst, 1983; Bothner-By et al., 1984) spectra were recorded by standard techniques using presaturation of the water signal and the time-proportional phase incrementation mode. A mixing time of 200 ms was used for NOESY and ROESY spectra. TOCSY spectra were recorded using 80 ms MLEV 16 with z-filter spin-lock sequence (Rance, 1987). Additional ROESY spectra were recorded on peptide samples in pure $D_2O$ to facilitate the observation of the CαH-CαH NOE cross-peaks close to the water signal. Acquisition data matrices were defined by 2,048 × 512 points in $t_2$ and $t_1$, respectively. Data were processed using the standard UXNMR Bruker programs on a Silicon Graphics computer. The 2D data matrix was multiplied by a square-sine-bell window function with the corresponding shift optimized for every spectrum and zero-filled to a 2K × 1K complex matrix prior to Fourier transformation. Baseline correction was applied in both dimensions.

Estimation of β-hairpin population was performed from the intensity of the CαH-CαH NOE characteristic of each β-hairpin, using as reference the intensity of an intraresidue CαH-Cα′H Gly NOE as described previously (Searle et al., 1995; de Alba et al., 1996, 1997; Ramírez-Alvarado et al., 1996). NOE intensities were measured by integration in ROESY spectra (100-ms mixing time) recorded in pure $D_2O$ samples.

### *Structure calculation*

Intensities of medium- and long-range NOEs were evaluated in a qualitative way and used to obtain upper limit distant constraints: strong (3 Å), intermediate between strong and medium (3.5 Å), medium (4 Å), intermediate between medium and weak (4.5 Å), weak (5 Å), and very weak (5.5 Å). Pseudo atom corrections were added where necessary. φ Angles were constrained to the range 0° to −180°, except for Gly. For those residues with $^3J_{C\alpha H\text{-}NH} > 7.9$ Hz, φ angles were restricted to the range −160° to −80°.

Structures were calculated on a Silicon Graphics computer using the program DIANA (Günter et al., 1991).

### *Protein structure database analysis*

The protein structure database used is implemented in the program WHATIF (Vriend, 1990). It includes 285 proteins with less than 50% homology. β-Hairpins were searched with the option scan 3D, which uses the Kabsch and Sander (1983) definition of secondary structure. A sequence length of 10 residues, 6 for the β-strands and 4 for the turn, was used to define β-hairpin 4:4 conformation. The turn region was restricted to be of type I. For the search of β-hairpins 3:5, a sequence length of 11 residues was used, from which 5 belong to the turn and 6 to the β-strands. Residues 4–7 were restricted to a type I turn. All the protein fragments given as output were visually inspected using the graphic system included in the program and were classified as β-hairpins 4:4 or 3:5 according to their expected structures (Sibanda & Thornton, 1991).

### *Estimation of hydrophobic surface area buried upon β-hairpin formation*

In order to estimate the hydrophobic surface area buried in protein β-hairpins 3:5 and 4:4, 10 β-hairpins of each type were selected randomly from the WHATIF protein database (Vriend, 1990) with those containing Cys or Pro in their sequences excluded for the analysis. The following protein β-hairpins 3:5 were used (Brookhaven Protein Data Bank codes are given in parentheses): 43–53 (135l), 71–81 (1lid), 42–52 (1nar), 17–27 (3lzm), 196–206 (2msb), 74–84 (1bfg), 231–241 (1gof), 9–19 (6tmn), 266–276 (1coy), and 193–203 (1cpn). The selected protein β-hairpins 4:4 were: 107–116 (1arb), 65–74 (1bfg), 7–16 (1frd), 57–66 (1pgx), 95–104 (3cla), 312–321 (3psg), 165–174 (2ltn), 73–82 (5rub), 303–312 (1nsc), and 252–261 (1gof). These β-hairpins were considered in isolation to calculate the hydrophobic surface area buried, which was computed as the difference between the solvent-accessible apolar surface area of the random structure and the ASA obtained for the structures of the selected β-hairpins 3:5 or 4:4. The solvent ASAs of the random structures were obtained by generating a total of 10 random structures for each hairpin sequence using the program SYBYL and averaging the ASAs calculated for each random structure. Solvent ASAs were calculated using the program VADAR (Wishart et al., 1993). The range of hydrophobic surface area buried upon β-hairpin 3:5 formation in proteins is 269–479 Å$^2$ (average 338 Å$^2$) and, upon β-hairpin 4:4 formation, the range is 200–341 Å$^2$ (average 266 Å$^2$).

## Supplementary material in Electronic Appendix

Tables SM1–SM6 list the δ values of peptides 2–7 and Tables SM7–SM12 list the nonsequential NOEs observed for peptides 2–7.

## Acknowledgments

We thank Mrs. C. López, Mr. A. Gómez, and Mr. L. de la Vega for their technical assistance and Dr. G. Rivas and Mr. J.A. Evangelio for their help in the use of the Beckman Optima XL-A ultracentrifuge. We are grateful to Dr. S. Padmanabhan for his suggestions concerning peptide synthesis and for his critical reading of the manuscript. This work was supported by the Spanish DGYCT project no PB93-0189. E.d.A. was the recipient of a predoctoral fellowship (AP93-51400679) from the Spanish Ministerio de Educación y Cultura.

## References

Atherton E, Sheppard RC. 1989. *Solid phase peptide synthesis: A practical approach*. Oxford: IRL Press.

Baldwin RL. 1995. α-Helix formation by peptides of defined sequence. *Biophys Chem 55*:127–135.

Blanco FJ, Jiménez MA, Herranz J, Rico M, Santoro J, Nieto JL. 1993. NMR evidence of a short linear peptide that folds into a β-hairpin in aqueous solution. *J Am Chem Soc 115*:5887–5888.

Blanco FJ, Jiménez MA, Pineda A, Rico M, Santoro J, Nieto JL. 1994a. NMR solution structure of the isolated N-terminal fragment of protein-G B1 domain. Evidence of trifluorethanol induced native-like β-hairpin formation. *Biochemistry 33*:6004–6014.

Blanco FJ, Rivas G, Serrano L. 1994b. A short linear peptide that folds into a native stable β-hairpin in aqueous solution. *Nature Struct Biol 1*:584–590.

Bothner-By AA, Stephens RL, Lee JM, Warren CD, Jeanloz RW. 1984. Structure determination of a tetrasaccharide: Transient nuclear Overhauser effects in the rotating frame. *J Am Chem Soc 106*:811–813.

Braunschweiler L, Ernst RR. 1983. Coherence transfer by isotropic mixing: Application to proton correlation spectroscopy. *J Magn Reson 53*:521–528.

Bundi A, Wuthrich K. 1979. $^1$H NMR parameters of the common amino acid residues measured in aqueous solution of linear tetrapeptides H-Gly-Gly-X-Ala-OH. *Biopolymers 18*:285–297.

Case DA, Dyson HJ, Wright PE. 1994. Use of chemical shifts and coupling constants in nuclear magnetic resonance structural studies on peptides and proteins. *Methods Enzymol 239*:392–416.

Chan AW, Hutchinson EG, Harris D, Thornton JH. 1993. Identification, classification, and analysis of β-bulges in proteins. *Protein Sci 2*:1574–1590.

Chou KC, Némethy G, Pottle MS, Scheraga HA. 1985. Folding of the twisted β-sheet in bovine pancreatic trypsin inhibitor. *Biochemistry 24*:7948–7953.

Chou PY, Fasman GD. 1974. Conformational parameters for amino acids in helical, β-sheet, and random coil regions calculated from proteins. *Biochemistry 13*:211–222.

Coste J, Le-Nguyen D, Castro B. 1990. PyBOP®: A new peptide coupling reagent devoid of toxic by-product. *Tetrahedron Lett 31*:205–208.

Cox JPL, Evans PA, Packman LC, Williams DH, Woolfson DN. 1993. Dissecting the structure of a partially folded protein. Circular dichroism and nuclear magnetic resonance studies of peptides from ubiquitin. *J Mol Biol 234*:483–492.

de Alba E, Blanco FJ, Jiménez MA, Rico M, Nieto JL. 1995. Interactions responsible for the pH dependence of the β-hairpin conformational population formed by a designed linear peptide. *Eur J Biochem 233*:283–292.

de Alba E, Jiménez MA, Rico M. 1997. Turn residue sequence determines β-hairpin conformation in designed peptides. *J Am Chem Soc 119*:175–183.

de Alba E, Jiménez MA, Rico M, Nieto JL. 1996. $^1$H NMR conformational investigation of designed short linear peptides able to fold into β-hairpin structures in aqueous solution. *Folding & Design 1*:133–144.

Dyson HJ, Wright PE. 1991. Defining solution conformations of small linear peptides. *Annu Rev Biophys Chem 20*:519–538.

Dyson HJ, Wright PE. 1993. Peptide conformation and protein folding. *Curr Opin Struct Biol 3*:60–65.

Günter P, Braun W, Wüthrich K. 1991. Efficient computation of three-dimensional protein structures in solution from nuclear magnetic resonance data using the program DIANA and the supporting programs CALIBA, HABAS and GLOMSA. *J Mol Biol 217*:517–530.

Haque TS, Gellman SH. 1997. Insights on β-hairpin stability in aqueous solution from peptides with enforced type I′ and type II′ β-turns. *J Am Chem Soc 119*:3301–3302.

Haque TS, Little JC, Gellman SH. 1994. "Mirror image" reverse turns promote β-hairpin formation. *J Am Chem Soc 116*:4105–4106.

Haque TS, Little JC, Gellman SH. 1996. Stereochemical requirements for β-hairpin formation: Model studies with four-residue peptides and depsipeptides. *J Am Chem Soc 118*:6975–6985.

Jeener J, Meier BH, Bachmann P, Ernst RA. 1979. Investigation of exchange processes by two-dimensional NMR spectroscopy.*J Chem Phys 71*:4546–4553.

Kabsch W, Sander C. 1983. Dictionary of protein secondary structure: Pattern recognition of hydrogen-bonded and geometrical features. *Biopolymers 22*:2577–2637.

Kim CA, Berg JM. 1993. Thermodynamic β-sheet propensities measured using a zinc-finger host peptide. *Nature 362*:267–270.

Kim PS, Baldwin RL. 1990. Intermediates in the folding reactions of small proteins. *Annu Rev Biochem 59*:631–660.

Kumar A, Ernst RR, Wüthrich K. 1980. A two-dimensional nuclear Overhauser enhancement (2D NOE) experiment for the elucidation of complete proton–proton cross-relaxation networks in biological macromolecules. *Biochem Biophys Res Commun 95*:1–6.

LaBrenz SR, Kelly JW. 1995. Peptidomimetic host that binds a peptide guest affording a $\beta$-sheet structure that subsequently self-assembles. A simple receptor mimic. *J Am Chem Soc 117*:1655–1656.

Lasters I, Wodak SJ, Alard P, van Custem E. 1988. Structural principles of parallel $\beta$-barrels in proteins. *Proc Natl Acad Sci USA 85*:3338–3342.

Laue TM, Shak BD, Ridgeway TM, Pelletier SL. 1992. Computer-aided interpretation of analytical sedimentation data for proteins. In: Harding SE, Rowe AJ, Horton JC, eds. *Analytical ultracentrifugation in biochemistry and polymer science*. Cambridge: Royal Society of Chemistry. pp 90–125.

Lyu PC, Wemmer DE, Zhou HX, Pinker RJ, Kallenbach NR. 1993. Capping interactions in isolated $\alpha$-helices: Position-dependent substitution effects and structure of a serine-capped peptide helix. *Biochemistry 32*:421–425.

Minor DL Jr, Kim PS. 1994a. Measurement of the $\beta$-sheet-forming propensities of amino acids. *Nature 367*:660–663.

Minor DL Jr, Kim PS. 1994b. Context is a major determinant of $\beta$-sheet propensity. *Nature 371*:264–267.

Muñoz V, Serrano L. 1994a. Elucidating the folding problem of helical peptides using empirical parameters. *Nature Struct Biol 1*:399–409.

Muñoz V, Serrano L. 1994b. Intrinsic secondary structure propensities of the amino acids, using statistical $\phi$-$\psi$ matrices: Comparison with experimental scales. *Proteins Struct Funct Genet 20*:301–311.

Nesloney CL, Kelly JW. 1996. A 2,3′-substituted biphenyl-based amino acid facilitates the formation of a monomeric $\beta$-hairpin-like structure in aqueous solution at elevated temperature. *J Am Chem Soc 118*:5836–5845.

Nowick JS, Holmes DL, Mackin G, Noronha G, Shaka AJ, Smith EM. 1996a. An artificial $\beta$-sheet comprising a molecular scaffold, a $\beta$-strand mimic, and a peptide strand. *J Am Chem Soc 118*:2764–2765.

Nowick JS, Mahrus S, Smith EM, Ziller JW. 1996b. Triurea derivatives of diethylenetriamine as potential templates for the formation of artificial $\beta$-sheets. *J Am Chem Soc 118*:1066–1072.

Ramírez-Alvarado M, Blanco FJ, Serrano L. 1996. De novo design and structural analysis of a model $\beta$-hairpin peptide system. *Nature Struct Biol 3*:604–612.

Rance M. 1987. Improved techniques for homonuclear rotating-frame and isotropic mixing experiments. *J Magn Reson 74*:557–564.

Searle MS, Williams DH, Packman LC. 1995. A short linear peptide derived from the N-terminal sequence of ubiquitin folds into a water-stable non-native $\beta$-hairpin. *Nature Struct Biol 2*:999–1006.

Searle MS, Zerella R, Williams DH, Packman LC. 1996. Native-like $\beta$-hairpin structure in an isolated fragment from ferredoxin: NMR and CD studies of solvent effects on the N-terminal 20 residues. *Protein Eng 9*:559–565.

Scholtz JM, Baldwin RL. 1992. The mechanism of $\alpha$-helix formation by peptides. *Annu Rev Biophys Biomol Struct 21*:95–118.

Sibanda BL, Blundell TL, Thornton JM. 1989. Conformation of $\beta$-hairpins in protein structures. A systematic classification with applications to modelling by homology, electron density fitting and protein engineering. *J Mol Biol 206*:759–777.

Sibanda BL, Thornton JM. 1985. $\beta$-Hairpin families in globular proteins. *Nature 316*:170–174.

Sibanda BL, Thornton JM. 1991. Conformation of $\beta$-hairpins in protein structures. Classification and diversity in homologous structures. *Methods Enzymol 202*:59–82.

Smith CK, Regan L. 1995. Guidelines for protein design. The energetics of $\beta$-sheet side chain interactions. *Science 270*:980–982.

Smith CK, Withka JM, Regan L. 1994. A thermodynamic scale for the $\beta$-sheet forming tendencies of amino acids. *Biochemistry 33*:5510–5517.

Swindells MB, MacArthur MW, Thornton JM. 1995. Intrinsic $\phi$, $\psi$ propensities of amino acids, derived from the coil regions of known structures. *Nature Struct Biol 2*:596–603.

Vriend G. 1990. WHATIF: A molecular modelling and drug design program. *J Mol Graph 8*:52–56.

Wang L, O'Connell T, Tropsha A, Hermans J. 1996. Molecular simulations of $\beta$-sheet twisting. *J Mol Biol 262*:283–293.

Wishart DS, Sykes BD. 1994. Chemical shifts as a tool for structure determination. *Methods Enzymol 239*:363–392.

Wishart DS, Willard L, Sykes BD. 1993. VADAR. *Volume angles define-s area, version 0.9*. Edmonton: University of Alberta. Protein Engineering Network of Centres of Excellence.

Wouters MA, Curmi PM. 1995. An analysis of side chain interactions and pair correlations within antiparallel $\beta$-sheets: The differences between backbone hydrogen-bonded and non-hydrogen-bonded residue pairs. *Proteins Struct Funct Genet 22*:119–131.

Wüthrich K. 1986. *NMR of proteins and nucleic acids*. New York: J. Wiley & Sons.

Wüthrich K, Billeter M, Braun W. 1984. Polypeptide secondary structure determination by nuclear magnetic resonance observation of short proton–proton distances. *J Mol Biol 180*:715–740.

Zhou HX, Lyu P, Wemmer DE, Kallenbach NR. 1994. Alpha helix capping in synthetic model peptides by reciprocal side chain-main chain interactions: Evidence for an N-terminal capping box. *Proteins Struct Funct Genet 18*:1–7.

Zhou NE, Kay CM, Sykes BD, Hodges RS. 1993. A single-stranded amphipathic alpha-helix in aqueous solution: Design, structural characterization, and its application for determining alpha-helical propensities of amino acids. *Biochemistry 32*:6190–6197.